Ions in water: From ion clustering to crystal nucleation

José Alejandre[1,2,*] and Jean-Pierre Hansen[2]
[1]*Departamento de Química, Universidad Autónoma Metropolitana-Iztapalapa, Av. San Rafael Atlixco 186, Col. Vicentina, 09340 Mexico D.F., Mexico*
[2]*Department of Chemistry, University of Cambridge, Lensfield Road, Cambridge CB2 1EW, United Kingdom*
(Received 14 August 2007; published 14 December 2007)

The clustering and nucleation of ions in aqueous solutions results from a competition between ion hydration and association. Molecular dynamics simulations of aqueous NaCl solutions are used to investigate ion clustering with a force field adjusted to reproduce experimental properties of the pure NaCl crystal and melt, and of concentrated solutions. The simulation results point to strong sensitivity of the nucleation mechanism to small changes in the force field. We report the numerical evidence for rapid crystal nucleation near saturation or under supercritical conditions.

DOI: 10.1103/PhysRevE.76.061505 PACS number(s): 61.20.Qg, 64.60.Qb, 64.75.+g, 82.30.Nr

A clear understanding of the physical mechanisms and parameters which control the solubility, clustering, and eventual precipitation of ions in water is of crucial importance for a wide range of disciplines, including solution chemistry, electrochemistry, mineralogy, geochemistry, and molecular biology. Applications range from colloid stability, biomolecular aggregation, and protein crystallization to corrosion, mineral dissolution, or hydrothermal ore deposition. Crude estimates, based on the Born model, relate the solubility to ion radii and solvent permittivity [1], but totally ignore the molecular nature of the solvent as well as ion-solvent coupling. Recent explicit free energy calculations via molecular dynamics (MD) simulations predict solubilities of alkali halide salts in water in reasonable agreement with experimental data [2,3]. Related simulations focus on ion hydration and the degree of ion association under ambient or high temperature and supercritical conditions [4–6], where ion clustering becomes predominant [7]. Experimental diagnostics of ion hydration, pairing and clustering include neutron diffraction [8,9], extended x-ray absorption fine structure (EXAFS) measurements [10], x-ray Compton scattering [11], as well as IR absorption and Raman scattering [12].

When solute saturation is reached, ion crystal nucleation and precipitation set in, which is the basis of important geological and industrial processes [13]. Supersaturation is achieved by increasing salt concentration, or increasing the temperature and pressure (hydrothermal conditions). Even below the saturation threshold an increase of temperature enhances ion clustering [5–7], as one would qualitatively expect from the concomitant drop in solvent permittivity. The initial stages of nucleation in a supersaturated aqueous solution have recently been observed in MD simulations [14], while the reverse process of the dissolution of an NaCl nanocrystal in water has also been studied by MD [15]. However, simulations have so far failed to yield clear evidence of nucleation of ion crystallites from an aqueous solution, contrary to the case of crystal nucleation from an ionic melt [16]. In this work we investigate ion clustering and nucleation in aqueous solutions, both under ambient and supercritical conditions, by MD simulations based on a generic force field, and report the numerical evidence for rapid crystal nucleation near saturation.

All simulations reported in this work were based on classical molecular dynamics (MD), using the velocity Verlet algorithm [17] to integrate the classical equations of motion. To properly account for the long range interactions, Ewald summations over periodic replicas of the basic simulation cell were carried out both for the Coulomb and Lennard-Jones forces [18,19]. Constant volume and temperature (*NVT*) or constant pressure and temperature (*NPT*) MD simulations [17,20] were performed on pure NaCl and aqueous solutions. *NPT* simulations of pure NaCl were carried out at zero pressure, using 1024 NaCl pairs in a cubic simulation cell. Bulk simulations of aqueous solutions involved a total of 500 particles (water molecules and Na or Cl ions); the number of NaCl pairs was varied between 0 and 50 to span molal concentrations from the dilute to the supersaturated regime. To simulate the liquid or vapour interface of a concentrated NaCl solution, 1260 water molecules and 120 NaCl pairs were placed in an elongated simulation cell with dimensions $L_x=L_y=26.3$ Å and $L_z=158$ Å surrounded by vaccum on both sides in the z direction [21].

The key input into any simulation is a reliable force field. A number of reasonably realistic pair potential models for pure water are available, but much of the existing literature on ionic solutions is based on the three-site, rigid SPC/E model [22]. This model involves a Lennard-Jones (LJ) potential between the oxygen sites and point charge Coulombic interactions between the O and H sites on different molecules, as shown in Eq. (1). The ion-water pair interaction has generally been fitted to the same functional form, involving a single point charge on the spherical ions and a LJ interaction between ion and O sites, so as to reproduce experimental data at low concentration [23–25]. It is then natural to adopt the same generic form (1) for the ion-ion interaction, rather than the Born-Huggins-Mayer form as parametrized by Tosi and Fumi [26], which has been widely used to describe pure salts (crystal and melt), in particular, for the determination of the liquid or vapor phase diagram [27] and melting curve [28] of alkali halides. The generic potential model used to describe aqueous NaCl solutions in the present work is hence

*Corresponding author. jra@xanum.uam.mx

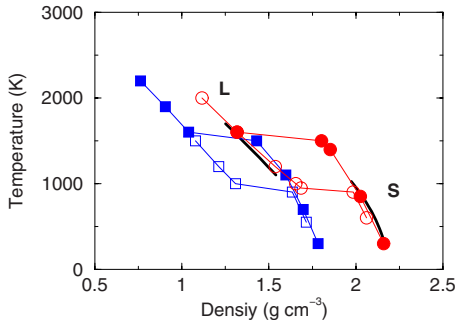

FIG. 1. (Color online) Liquid-solid phase diagram of pure NaCl. Solid continuous lines are experimental results for the liquid [27] and solid [29] phases. (*NPT*) MD results from this work use σ_{ClCl} =4.401 Å (squares) and σ_{ClCl}=4.036 Å (circles). Filled and open symbols are for heating and cooling cycles, respectively.

$$u(r) = 4\epsilon_{\alpha\beta}\left[\left(\frac{\sigma_{\alpha\beta}}{r}\right)^{12} - \left(\frac{\sigma_{\alpha\beta}}{r}\right)^{6}\right] + \frac{1}{4\pi\epsilon_0}\frac{q_\alpha q_\beta}{r}, \qquad (1)$$

where r is the distance between sites α and β, q_α is the electric charge of site α, ϵ_0 is the permitivity of the vacuum, $\epsilon_{\alpha\beta}$ is the LJ energy scale, and $\sigma_{\alpha\beta}$ is the repulsive diameter for an $\alpha\beta$ pair, with α or β=O, H, Na, or Cl. The O-O, O-H, and H-H parameters are taken here from the standard SPC/E set, which assumes $\epsilon_{\mathrm{OH}}=\epsilon_{\mathrm{HH}}=0$ [22]. Within the same assumption, ϵ_{ClO}, σ_{ClO}, ϵ_{NaO}, and σ_{NaO} could be taken from the Dang fits to low concentration experimental data [24,25], while the ion-ion LJ parameters could finally be determined from the above by the Lorentz-Berthelot mixing rules as follows:

$$\sigma_{\alpha\beta} = \left(\frac{\sigma_{\alpha\alpha}+\sigma_{\beta\beta}}{2}\right), \quad \epsilon_{\alpha\beta} = (\epsilon_{\alpha\alpha}\epsilon_{\beta\beta})^{1/2}. \qquad (2)$$

However, the resulting ion-ion potentials do not yield an accurate description of the pure NaCl salt, as required for a realistic modeling of nucleation. In Fig. 1 we compare our MD results to experimental data [29] for crystal or melt coexistence, using the Dang ion-ion force field [25]. The MD results exhibit hysteresis between the liquidus and solidus (we made no attempt to determine the exact tie line by explicit free energy calculation of the two phases [28]), but the two branches are shifted to significantly lower densities compared to experiment. Good agreement with experiment, as ilustrated in Fig. 1, is restored by adjusting the LJ potential parameter σ_{ClCl} from 4.401 Å to 4.036 Å. This force field (model A) will marginally favor ion association over ion hydration compared to the Dang force field. It is the competition between the two mechanisms (association and hydration) which ultimately control the rate of nucleation. This competition is also regulated by the Cl-water interaction. While the cation Na^+ is repelled by the cationic water H-sites, so that there is no need to add a LJ interaction between Na and H sites on top of their Coulombic repulsion,

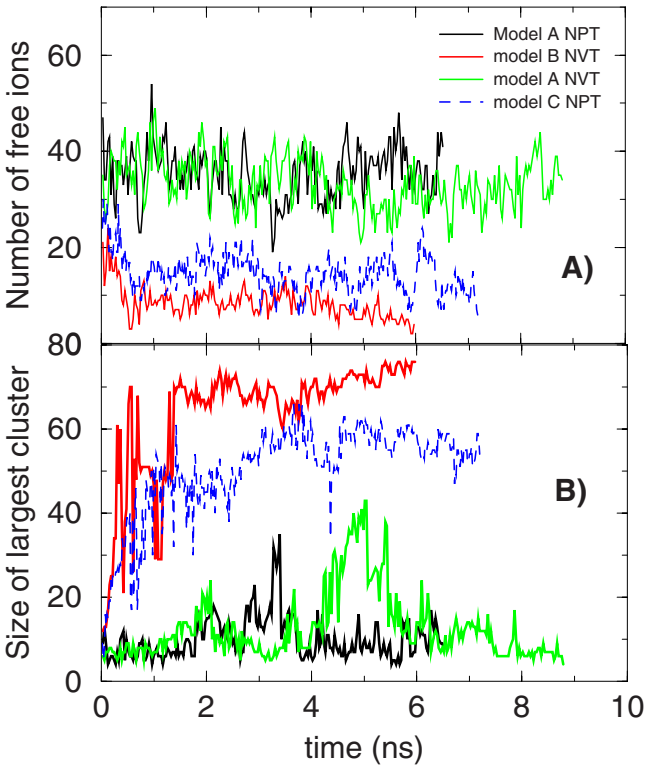

FIG. 2. (Color online) Clustering as a function of time in 5.3m solutions (40 NaCl pairs and 420 water molecules) at 300 K and ρ=1.17 g cm^{-3}. (a) Number of free ions. (b) Size of the largest cluster.

this is no longer true for the Cl-H interaction, because of the strong Coulombic attraction between the anion and the H sites of the water molecule. The Coulomb collapse is only prevented by the repulsive part of the LJ potential between O and Cl sites but this repulsion may not be sufficiently strong, and our LJ model combined with the Lorentz-Berthelot rules is thus expected to favor ion hydration over ion association, as a consequence of too strong Cl-H bonding. This trend is confirmed by long, room temperature MD simulations of our generic model (1), using the quoted LJ parameters. We use a simple geometric criterion (two ions belong to the same cluster if $r<3$ Å) to determine the number of free (unpaired) ions, as well as the size of the largest cluster, as functions of time. At low concentration most ions are seen to remain single throughout the run, while close to experimental saturation conditions the largest cluster contains only about 12% of all ions. The results for a 5.3 molal (m) ion concentration are shown in Fig. 2. Although the formation of larger clusters and eventual nucleation at even higher concentrations cannot be ruled out for the present model, the reluctance of ions to cluster points to a deficiency of our generic model A. The deficiency appears to lie in the excessive Cl-H bonding mentioned earlier. The simplest way to correct for this is to make a *nonadditivity* correction to the Lorentz rule for the Cl-O diameter, such that $\sigma_{\mathrm{ClO}}=(\sigma_{\mathrm{ClCl}}+\sigma_{\mathrm{OO}})(1+\Delta_{\mathrm{ClO}})/2$. With $\Delta_{\mathrm{ClO}}=0.02$ (model B), the fraction of *free* ions in a saturated solution drops rapidly below 10%, while a single large cluster forms simultaneously containing practically all the re-

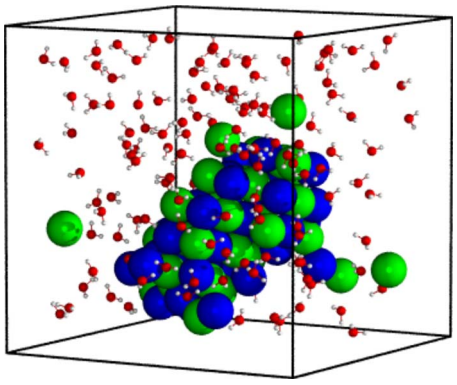

(a)

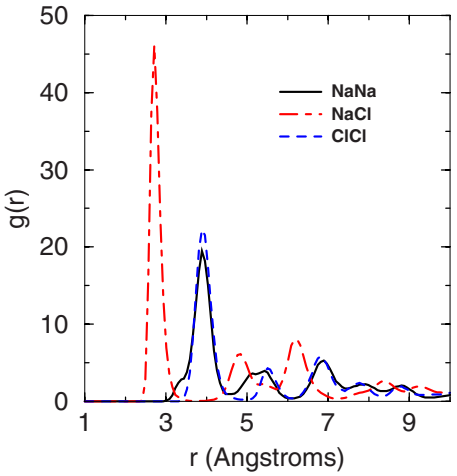

(b)

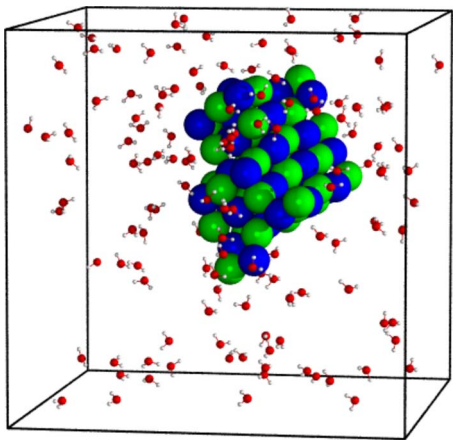

(c)

FIG. 3. (Color online) (a) Snapshot of 40 NaCl pairs in 420 water molecules at 300 K from an *NVT* MD simulation based on model B. The number and size of water molecules is strongly reduced for better visualization. (b) Radial distribution functions of ion-ion pairs at 300 K and 5.3*m* from *NVT* MD simulations using model B. (c) Snapshot of 40 NaCl pairs in 420 water molecules under supercritical conditions (T=683 K; ρ=0.35 g cm^{-3}) from *NVT* MD simulations based on model B.

maining ions, as shown in Fig. 2(b). Inspection of the cluster, a snapshot of which is shown in Fig. 3(a), indicates that it is an elongated crystallite with NaCl structure, as confirmed by

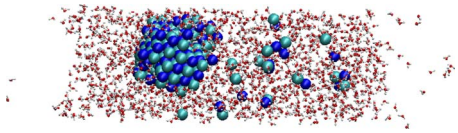

FIG. 4. (Color online) Snapshot of 120 NaCl pairs in 1260 water molecules in a liquid slab (see the main text), using model B.

the characteristic ionic radial distribution functions shown in Fig. 3(b).

The drawback of model B is that it tends to overestimate ion clustering at concentrations well below saturation. Thus, at a molal ion concentration of about 2.5 (20 NaCl pairs in 460 water molecules) at room temperature, the fraction of free ions is only about 25%, while the largest cluster contains about 50% of the ions after 3.6 ns. An alternative to balance the attractive electrostatic Cl-H interactions is to include an LJ potential between ions and the H atoms in water [23]. In addition to the parameters of model A, the new force field (model C) introduces σ_{HH}=0.65 Å and ϵ_{HH} =0.166 28 kJ mol^{-1} to calculate the cross interactions between ions and H by using Eq. (2). The H-H and H-O interactions remain purely electrostatic as in the SPC/E water model. Within model C, ion clustering is inhibited at room temperature below saturation, as ilustrated in Fig. 2(b), while under experimental saturation conditions, nucleation appears to be faster for model B than for model C. The variation of the density ρ of the solution with ion concentration follows the relation $\rho=0.9974+0.037m-0.00095m^2$ and agrees very well with experimental data under normal pressure.

We have extended the room temperature MD simulations to supercritical conditions (ρ=0.35 g cm^{-3}; T=683 K) using models B and C for a 5.3 molal salt concentration. Rapid ion clustering and eventual crystal nucleation (after 2 ns) was observed with model B. The nucleation process was slower with model C, with the crystallite structure appearing after 7.5 ns. In both cases, a single large compact cluster containing most of the 40 NaCl pairs was found [see Fig. 3(c)]. The radial distribution functions of the ion pairs are similar to those shown in Fig. 3(b).

In view of the recent interest in ions near the water liquid or vapor interface [30], which has implications in atmospheric science, we have also simulated NaCl solutions in a liquid slab in equilibrium with its vapor on both sides [21] at 500 K. A compact cluster developed in the liquid region in simulations using model B or C force fields. Inspection of the cluster shown in Fig. 4 and of the partial ion-ion pair distribution functions demostrate its crystalline structure. In view of the confinement by the two liquid or vapor interfaces, the observed clustering may be regarded as an example of heterogeneous nucleation.

We use a generic force field which has been validated against a number of thermodynamic properties of NaCl crystals and solutions. The generic force field *C* is thus seen to lead to rapid ion clustering and nucleation of ionic crystallites close to experimental saturation conditions over a range of temperatures, including supercritical conditions. The crystal nucleation process involves ion dehydration, i.e., the exclusion of water molecules from the inside of the observed

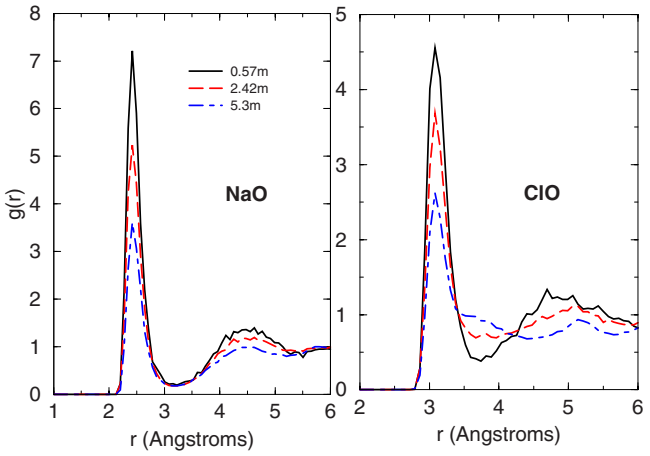

FIG. 5. (Color online) Pair distribution functions $g(r)$ of Na-O and Cl-O pairs at 300 K and at different molal concentrations using model C.

compact clusters and crystallites, as clearly diagnosed by the partial ion-oxygen pair distribution functions, shown in Fig. 5, which signal a dramatic drop of the water coordination number around ions. For example, the number of water molecules around the Cl ion varies from 6 at 0.57m to 2.5 at 5.3m at room temperature.

The key finding of our MD simulations is the extreme sensitivity of the observed clustering and nucleation to minute changes in the force field, which affect the delicate balance between ion hydration and ion association. In view of the strength of the bare Coulombic interactions between charged sites, small changes in the repulsive cores characterized by the $\sigma_{\alpha\beta}$ parameters in the LJ potential (1) lead to significant variations of the attractive energy between opposite charges at contact. The force fields developed in this work are not necessarily the most realistic, despite their consistency with relevant experimental data, but they are the first to lead to a rapid enhancement of ion association with concentration, and eventually to nucleation of NaCl crystallites over a broad range of physically reasonable conditions. Force field C appears to be superior to the nonadditive model B at low ion concentration, where the latter overestimates ion clustering, but both force fields yield very similar results near saturation. Our simulations pinpoint the key aspects of force fields which control clustering and nucleation. Quantitative estimates of nucleation rates require detailed estimates of free energy barriers and kinetic factors, as obtained in recent studies of crystal nucleation from quenched melts [16,31], but the results of the present simulations point to fast rates in the case of ionic solutions. Such solutions thus appear to be attractive model systems for a better understanding of homogeneous nucleation, an ubiquitous mechanism which has so far eluded quantitative agreement between simulation, theory, and experiment in the case of melts. The sensitivity of ion clustering and nucleation to small changes in the force field challenges the quantitative credibility of simulation results for more complex, biomolecular systems and processes, such as protein aggregation and crystallization controlled by salt concentration and hydration.

The authors thank F. Bresme, D. Heyes, and R. Lynden-Bell for a critical reading of the manuscript and constructive comments. J.A. is grateful to Schlumberger Cambridge Research for their support during his sabbatical visit to Cambridge.

[1] J. Israelachvili, *Intermolecular and Surface Forces*, 2nd ed. (Academic, London, 1992).
[2] M. Ferrario, G. Ciccoti, E. Spohr, T. Cartailler, and P. Turk, J. Chem. Phys. **117**, 4947 (2002).
[3] E. Sanz and C. Vega, J. Chem. Phys. **126**, 014507 (2007).
[4] J. P. Brodholt, Chem. Geol. **151**, 11 (1998).
[5] T. Driesner, T. M. Seward, and I. G. Tironi, Geochim. Cosmochim. Acta **62**, 3095 (1998).
[6] S. Koneshan and J. C. Rasaiah, J. Chem. Phys. **113**, 8125 (2000).
[7] E. H. Oelkers and H. C. Helgeson, Science **261**, 888 (1993).
[8] T. Yamaguchi, M. Yamagami, H. Ohzono, H. Wakita, and K. Yamaka, Chem. Phys. Lett. **252**, 317 (1996).
[9] S. Ansell and G. W. Neilson, J. Chem. Phys. **112**, 3942 (2000).
[10] T. M. Seward, C. M. B. Henderson, J. M. Charnock, and T. Driesner, Geochim. Cosmochim. Acta **63**, 2409 (1999).
[11] K. Nygard, M. Hakala, S. Manninen, K. Hamalainen, M. Itou, A. Andrejczuk, and Y. Sakurai, Phys. Rev. B **73**, 024208 (2006).
[12] G. V. Bondarenko, Y. E. Gorbaty, A. V. Okhulkov, and A. G. Kalinicher, J. Phys. Chem. A **110**, 4042 (2006).
[13] M. Hovland, T. Kuznetsova, H. Rueslatten, B. Kramme, H. K. Johnsen, G. E. Fladmark, and A. Heback, Basin Res. **18**, 221 (2006).
[14] D. Zahn, Phys. Rev. Lett. **92**, 040801 (2004).
[15] Y. Yang, S. Meng, L. F. Xu, E. G. Wang, and S. Gao, Phys. Rev. E **72**, 012602 (2005); J. Phys.: Condens. Matter **18**, 10165 (2006).
[16] C. E. Valeriani, E. Sanz, and D. Frenkel, J. Chem. Phys. **122**, 194501 (2003).
[17] D. Frenkel and B. Smit, *Understanding Molecular Simulation*, 2nd ed. (Academic, San Diego, 2002).
[18] U. Essmann, L. Perera, M. L. Berkowitz, T. Darden, H. Lee, and L. G. Pedersen, J. Chem. Phys. **103**, 8577 (1995).
[19] J. López-Lemus and J. Alejandre, Mol. Phys. **100**, 2983 (2002).
[20] M. E. Tuckerman, J. Alejandre, R. López-Rendón, A. L. Jochim, and G. J. Martyna, J. Phys. A **39**, 5629 (2006).
[21] J. Alejandre, G. A. Chapela, and D. J. Tildesly, J. Chem. Phys. **102**, 4574 (1995).
[22] H. J. C. Berendsen, J. R. Grigera, and T. P. Straatsma, J. Phys. Chem. **91**, 6269 (1987).
[23] B. M. Pettit and P. J. Rossky, J. Chem. Phys. **84**, 5836 (1986).
[24] D. E. Smith and L. X. Dang, J. Chem. Phys. **100**, 3757 (1994).
[25] L. X. Dang, J. Am. Chem. Soc. **117**, 6954 (1995).
[26] M. P. Tosi and F. G. Fumi, J. Phys. Chem. Solids **25**, 45

(1964).
[27] Y. Guissani and B. Guillot, J. Chem. Phys. **101**, 490 (1994).
[28] J. Anwar, D. Frenkel, and M. G. Noro, J. Chem. Phys. **118**, 728 (2003).
[29] J. O. M. Bockris, A. Pilla, and J. L. Barton, J. Phys. Chem. **64**, 507 (1960).
[30] B. C. Garret, Science **303**, 1146 (2004).
[31] S. Auer and D. Frenkel, Nature (London) **409**, 1020 (2001).